Joint Recovery of Two Carriers from One-bit Sampled Signals

Aparna Agrawal, Kumar Appaiah, Sibi Raj B. Pillai
Department of Electrical Engineering
Indian Institute of Technology Bombay, Mumbai, India

***Abstract*—Carrier frequency offset estimation is an essential component of receiver subsystems. In many scenarios such as Global Navigation Satellite Systems (GNSS) and multiband communication systems, multiple frequencies need to be estimated simultaneously. Frequency estimation involves a combination of analog and digital processing to estimate offsets in the presence of Doppler shifts. However, digital processing using high resolution analog to digital converters (ADCs) involves complex implementations. Recent work has demonstrated that carrier recovery can be performed with just sign discrimination of the received signal, thereby obviating the need for higher vertical resolution ADCs. In this paper, we present approaches to estimate two frequencies from one-bit samples in the presence of noise. We solve carrier recovery problem using spectral estimation by using their zero-crossings. The zero-crossings can be formulated as a non-uniformly sampled sinusoid recovery problem that can be solved using periodogram based approaches. Our algorithms yield accurate frequency and phase estimates simultaneously for multiple carriers that are robust to noise and sampling jitters.**

***Index Terms*—One-bit quantization, spectral analysis**

I. Introduction

CARRIER synchronization is an essential part of receiver subsystems in high frequency communication systems. Frequency offset occurs due to a combination of several effects, including differences in the reference frequencies at the transmitter and user equipment (UE) as well as Doppler shifts. Carrier recovery is typically performed using a combination of analog and digital approaches [1]. A coarse correction in the analog domain is followed by a fine carrier estimation and recovery using digital systems. Such approaches rely on analog to digital converters (ADCs) to sample the signal for further processing. Note that a larger vertical resolution for the ADC leads to higher complexity and power consumption [2]. In several communication systems, such as GNSS receivers, the structure of the transmitted signal is generally limited to being binary in nature. Past work has demonstrated that even when one-bit ADCs are used, efficient methods for carrier recovery exist [3]. In this paper, we consider the situation where we have only one-bit ADCs that produce single bit samples from the input signals, and show that two frequencies can be estimated simultaneously from one-bit ADC samples. The zero-crossings of the quantized waveform preserve their phase and frequency characteristics, since the signals that we consider are sinusoids with a well defined structure, enabling spectral estimation to recover these accurately.

The work of Sibi Raj B. Pillai and Kumar Appaiah was supported by a Qualcomm UR 6G grant.

Signal recovery using one-bit samples has been considered in several contexts in prior work. It is known that the lack of vertical resolution when using 1-bit ADCs or comparable simpler ADC designs can be compensated for using appropriate oversampling in the case of band-limited signals [2, 4–11]. Similarly, learning and compressive sensing based approaches for signal recovery have also garnered significant attention in past work [12]. A common thread among these approaches is that they largely aim to track phase differences between the single carrier reference and the received signal. On the other hand, we consider the recovery of multiple carriers simultaneously; that too, with one-bit samples [13, 14]. Several past approaches in this direction have presented zero-crossing counting based approaches [15, 16], although these are largely limited to recovering a single carrier. In our work, we demonstrate that through the use of effective spectral estimation techniques, computationally efficient methods are able to recover multiple carriers with phase, frequency and their relative amplitudes from noisy one-bit receptions. Our main contributions involve carrier recovery methods from 1-bit samples of a noisy received signal that contains two pure carriers. Our spectral estimation based methods are able to efficiently recover the two carriers with sufficient accuracy.

The rest of this paper is organized as follows: the System Model is described in Section II. The proposed carrier recovery methods for a noisy received signal consisting of two carriers are described in Section III. Simulation based evaluation of the proposed methods is discussed in Section IV. Finally, Section V summarizes the work and discusses future extensions.

II. System Model

We assume that the carriers are in the intermediate frequency range, which is typically between 100 kHz and 500 kHz for cellular systems, and around 10s of MHz for satellite receiver systems. Throughout, the sampling is assumed to satisfy the Nyquist criterion, i.e. the sampling rate f_s exceeds twice frequency of the largest carrier.

A. System model for two carrier received signal

For the problem of recovering two carriers at the receiver, we assume that the user equipment (UE) receives carriers from two different transmitters, with known nominal frequencies f_{c1}

and f_{c2}. We assume that the unknown frequency offsets (which we potentially attribute to sources like Doppler translation during propagation) from each of the two transmitters is f_{d1} and f_{d2} respectively, and the initial phases with which the two carriers are received are θ_1 and θ_2 respectively. We assume that the continuous-time received signal is of the form

$$r(t) = \text{sign}\big(A_1 s_1(t) + A_2 s_2(t) + w(t)\big), \tag{1}$$

where $s_i(t) = \cos(2\pi(f_{ci} + f_{di})t + \theta_i)$ and $w(t)$ is the additive noise process. Since the UE is equipped with only a one-bit ADC, the sampled received signal $r[n] \triangleq r(nT_s)$ is:

$$r[n] = \text{sign}\left(A_1 s_1[n] + A_2 s_2[n] + w[n]\right). \tag{2}$$

Here, the operator $\text{sign}(x)$ returns 1 if $x \geq 0$ and -1 otherwise. The additive noise $w[n]$ is independent and identically distributed, according to a zero mean white Gaussian noise with variance $\frac{N_0}{2}$. Without loss of generality, we assume the amplitudes obey $|A_2| \leq |A_1|$, hence we will term the first transmission as the stronger one and take $A_1 = 1$ and $|A_2| \leq 1$. We further assume $A_2 > 0$ as we account for the sign difference in the phase of $s_2(t)$, θ_2. Typically, the transmission would also be affected by the effective channel between the transmitter and UE; we assume that the tuple $(\theta_1, \theta_2, A_2)$ accounts for the effects of the medium.

We remark here that the signal model in (2) is quite general when the UE receives only the carrier, since the amplitude and phase changes during propagation through a channel are captured within the parameters f_{d1}, f_{d2}, θ_1, θ_2 and A_2. Thus, the model is valid as long as these parameters can be assumed to be constant and not undergo significant changes in the duration of the carrier recovery process. In addition, the sign operator on a sinusoid introduces odd harmonics of the fundamental frequency. Thus, if A_2 is small and $(f_{c2} + f_{d2}) = (2N - 1)(f_{c1} + f_{d1})$ for a positive integer N, the joint recovery problem becomes ill-defined. Clearly, the chances of this situation are very low in practical scenarios.

B. Spectral Estimation under Non-uniform Sampling

The Lomb-Scargle periodogram [17] can be used to obtain frequency content of the signal from its irregularly spaced apart samples. It applies least-squares regression and fits a combination of sinusoids directly onto the data. The quality of the fit is determined by the spectral power at that frequency, and the most dominant frequency candidate is chosen. This approach is robust to noise since it performs the fit across all data points, essentially averaging out the noise. Further, the amplitude A and phase θ are jointly extracted by computing the complex correlation Z between the received non-uniform samples at t_l instants given by $As(t_l)$ where $s(t_l) = \cos(2\pi f_d t_l + \theta)$ and a complex exponential at frequency f_d. This is expressed as $Z = \sum_{l=1}^{N} A\, s(t_l) e^{-j2\pi f_d t_l}$, where the amplitude is $A = \frac{2}{N}|Z|$ and the phase is $\theta = \arg(Z)$. One aspect to note is that this approach would yield (f_d, θ) and $(-f_d, -\theta)$ as candidate solutions due to the ambiguity in the sign of the cosine. However, we can disambiguate these using back substitution in order to obtain the correct solution.

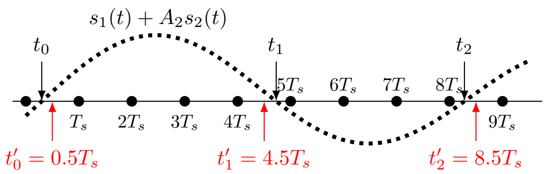

Fig. 1. Zero-crossings of $r[n]$ and its estimates.

III. Recovering two carriers with one-bit samples

In this section, we outline the carrier recovery using one-bit samples. We develop a robust approach that connects the phases of $s_1[n]$ and $s_2[n]$ with the zero-crossings of $r[n]$ to estimate the parameters $(f_{d1}, f_{d2}, \theta_1, \theta_2)$. We first present the analysis of the zero-crossings of the received signal.

A. Zero-crossing uncertainty due to jitter

An analog discriminator, in the absence of noise, provides the accurate location of the zero-crossings of $r(t)$. However, since we only have access to the sampled version of $r(t)$, the precise zero-crossing locations are not available. Notice that zero-crossings lie between any pair of consecutive time instants within which $r[n]$ changes sign. For the sign changing between $r[n]$ and $r[n+1]$, we mark $(n + \frac{1}{2})T_s$ as the zero-crossing instant. Let $t'_0, t'_1, \dots$ denote the sequence of zero-crossing instants thus generated. Let t_k be the actual zero-crossing instant of $r(t)$ that is closest to t'_k. We then have

$$\max |t'_k - t_k| = 1/(2f_s). \tag{3}$$

B. Recovery of carriers

We now formulate the recovery problem for the two carriers with $A_2 \in (0, 1)$ using both linear and non-linear approaches for estimating the frequency offsets, phases and relative amplitude. Since the one-bit samples can be thought to have been obtained by sampling the received signal after passing it through a comparator, we first formulate our equations in the continuous-time, and subsequently provide their sampled versions. Let us rewrite the signal $s_2(t)$ as $s_2(t) = \cos(2\pi(f_{c2} + f_{d2} - f_{c1})t + \theta_2 + 2\pi f_{c1} t)$. Now, using standard trigonometric identities, we get

$$\begin{aligned} s_1(t) + A_2 s_2(t) = \cos(2\pi f_{c1} t)\big[&\cos(2\pi f_{d1} t + \theta_1) \\ &+ A_2 \cos(2\pi(f_{c2} + f_{d2} - f_{c1})t + \theta_2)\big] \\ &- \sin(2\pi f_{c1} t)\big[\sin(2\pi f_{d1} t + \theta_1) \\ &+ A_2 \sin(2\pi(f_{c2} + f_{d2} - f_{c1})t + \theta_2)\big]. \end{aligned}$$

Hence, we can express the continuous-time received signal as

$$r(t) = \text{sign}\left(R(t)\cos(2\pi f_{c1} t + \phi_1(t)) + w(t)\right), \tag{4}$$

where, denoting $f_{c2} - f_{c1}$ as Δ_f, we have

$$\tan\phi_1(t) = \frac{\sin(2\pi f_{d1} t + \theta_1) + A_2 \sin(2\pi(\Delta_f + f_{d2})t + \theta_2)}{\cos(2\pi f_{d1} t + \theta_1) + A_2 \cos(2\pi(\Delta_f + f_{d2})t + \theta_2)}$$

$$R(t) = \sqrt{1 + A_2^2 + 2A_2 \cos(2\pi(\Delta_f + f_{d2} - f_{d1})t + \theta_2 - \theta_1)}.$$

Substituting $\alpha(t) \triangleq (2\pi f_{d1}t + \theta_1) \pmod{2\pi}$ and $\beta(t) \triangleq (2\pi f_{d2}t + \theta_2) \pmod{2\pi}$, we express $\tan\phi_1(t)$ and $R(t)$ as:

$$\tan\phi_1(t) = \frac{\sin\alpha(t) + A_2 \sin\left(2\pi\Delta_f t + \beta(t)\right)}{\cos\alpha(t) + A_2 \cos\left(2\pi\Delta_f t + \beta(t)\right)}, \tag{5}$$
$$R(t) = \sqrt{1 + A_2^2 + 2A_2\cos(2\pi\Delta_f t + \beta(t) - \alpha(t))}.$$

Let us now exploit the information from the sign transitions in $r(t)$ to estimate the unknown frequency offsets and phases. The magnitude $R(t)$ remains positive (in fact, bounded away from 0 since we assumed $A_2 < 1$), and thus, the zero-crossing transitions in $r(t)$ can be attributed solely to the cosine component in (4). In the absence of noise, when $r(t)$ transitions from positive to negative, the phase of the cosine at the precise transition time is $2m\pi + \pi/2$ for some integer m. Conversely, when $r(t)$ transitions from negative to positive, the phase corresponds to $2m\pi + 3\pi/2$. From the zero-crossing instants of $r(t)$, labeled as $t_k, k \geq 0$, the phase of $r(t_k)$ is:

$$\phi(t_k) \triangleq \begin{cases} 2m\pi + \pi/2 - 2\pi f_{c1}t_k, & r(t_k+\delta) - r(t_k - \delta) < 0 \\ 2m\pi + 3\pi/2 - 2\pi f_{c1}t_k, & r(t_k+\delta) - r(t_k - \delta) > 0, \end{cases} \tag{6}$$

where $0 < \delta < T_s/2$. Using (5) – (6), we can now form a set of equations that can be solved by a non-linear solver as described below.

1) Non-Linear Solver: At each zero-crossing instant t_k, we have $\alpha(t_k)$, $\beta(t_k)$ and A_2 as unknowns. Using (5), we can get an independent equation for each t_k as

$$\phi_1(t_k) = \tan^{-1}\left[\frac{\sin\alpha(t_k) + A_2 \sin\left(2\pi\Delta_f t_k + \beta(t_k)\right)}{\cos\alpha(t_k) + A_2 \cos\left(2\pi\Delta_f t_k + \beta(t_k)\right)}\right]. \tag{7}$$

Three consecutive zero-crossing instants can now be used to estimate the three unknowns, as the value of $\alpha(t_k)$ and $\beta(t_k)$, which are determined by f_{d1} and f_{d2}, do not vary significantly within the interval $[t_k, t_{k+2}]$. Therefore, we take

$$\alpha(t_k) \approx \alpha(t_{k+1}) \approx \alpha(t_{k+2}),$$
$$\beta(t_k) \approx \beta(t_{k+1}) \approx \beta(t_{k+2}). \tag{8}$$

We can uniquely determine the value and quadrant of $\alpha(t_k)$ and $\beta(t_k)$ from the tuple $(\phi_1(t_k), \phi_1(t_{k+1}), \phi_1(t_{k+2}))$ obtained from three consecutive zero-crossing measurements. Since $\phi_1(t_k)$ defined in (7) is non-linear in $\alpha(t_k)$ and $\beta(t_k)$, an appropriate non-linear solver is required. For example, the least-squares regression method from the SciPy software library can be employed for this estimation [18]. Recall that both $\alpha(\cdot)$ and $\beta(\cdot)$ are periodic with period 2π. Since $\alpha(\cdot)$ and $\beta(\cdot)$ vary slowly over time, we can refine the estimates using subsequent tuples of zero-crossing measurements. Our estimation steps involve finding A_2 by averaging the estimates of $A_2(t_k)$ over t_k, and estimating f_{d1} and f_{d2} from $\alpha(\cdot)$ and $\beta(\cdot)$. One approach for this is to unwrap the latter as phases (since they are modulo 2π) and use a linear-fit to estimate the Doppler frequencies from their slopes, and the corresponding phase offsets from the intercept.

Remark 1. *As an alternative to the last step, we can employ the Lomb-Scargle periodogram over $\cos\alpha(t)$ and $\cos\beta(t)$ to obtain f_{d1} and f_{d2} from the non-uniformly spaced samples as discussed in Section II-B.*

Notice that while using the sampled version of $r(t)$, denoted as $r[n] = r(nT_s)$, we do not have precise zero-crossing instances of $r(t)$, as discussed in Section III-A, and thus, we assume that the zero-crossings are the mid-point between the sampled locations that has a transition in the sign of $r[n]$, labeled t'_k. These temporal estimates may cause additional errors in the estimates of $\{\alpha(t'_k), \beta(t'_k), A_2(t'_k)\}$, be it the phase unwrapping solution or the periodogram based approach. For the former, the zero-crossing jitter calls for further smoothening of the estimates before phase unwrapping.

The operational complexity of the Lomb-Scargle periodogram depends on the number of observed data points and the number of frequencies in search grid. Hence, the complexity of this method depends on the number of zero-crossings under consideration over which the non-linear solver is used. The complexity is given by $O(K \cdot F_{\text{search}})$ where K is the number of zero-crossings under consideration and F_{search} are the number of frequencies in the search space.

2) Linear Solver: We now present an alternate approach that involves formulation of the frequency estimation problem as a system of linear equations. We define the vector $\vec{w}(t)$ as

$$\vec{w}(t) = \left[\sin\alpha(t)\,,\, \cos\alpha(t)\,,\, A_2\sin\beta(t)\,,\, A_2\cos\beta(t)\right]^T,$$

with $w_i(t)$ denoting the i-the entry. Notice from (5) that

$$\tan\phi_1(t)\left[w_2(t) + \cos(2\pi\Delta_f t)w_4(t) - \sin(2\pi\Delta_f t)w_3(t)\right]$$
$$= w_1(t) + \sin(2\pi\Delta_f t)w_4(t) + \cos(2\pi\Delta_f t)w_3(t), \tag{9}$$

which is linear in $\vec{w}(t)$. Using the slowly varying assumption in (8), from three consecutive zero-crossing measurements, viz. (t_k, t_{k+1}, t_{k+2}), we can form a set of linear equations,

$$M(t)\vec{w}(t) = \vec{0}, \tag{10}$$

where $M(t)$ is defined as:

$$M(t) = \begin{bmatrix} 1 & -T_1 & c_1 + s_1T_1 & s_1 - c_1T_1 \\ 1 & -T_2 & c_2 + s_2T_2 & s_2 - c_2T_2 \\ 1 & -T_3 & c_3 + s_3T_3 & s_3 - c_3T_3 \end{bmatrix}.$$

Here, we have denoted $T_i \triangleq \tan(\phi_1(t_{k-1+i}))$, $c_i \triangleq \cos(2\pi\Delta_f t_{k-1+i})$ and $s_i \triangleq \sin(2\pi\Delta_f t_{k-1+i})$. While this gives us three equations for four variables, the fact that $|w_1(t)|^2 + |w_2(t)|^2 = 1$ naturally constrains the solution set. The null space of $M(t)$, denoted as $\vec{w_0}(t)$, is the required scaled solution, except in ill-conditioned situations where the kernel dimension is more than one. Since $|w_1(t)|^2 + |w_2(t)|^2 = 1$, the actual solution is of the form $\vec{w}(t) = \lambda(t)\vec{w_0}(t)$, where $\lambda(t) = \pm 1/(\sqrt{|w_{01}(t)|^2 + |w_{02}(t)|^2})$.

Using (6) and the nominal carrier frequencies, we can evaluate T_i, c_i and s_i respectively at the different zero-crossing instants of $r(t)$. Utilizing these constants, we can solve (10) under the constraint and obtain the solution as

$\vec{w}(t) = \lambda(t)\vec{w_0}(t)$. The resulting solution contains a directional ambiguity. Since the sign of $\lambda(t)$ is undetermined, the final vector could be expressed as either $\vec{w}(t)$ or $-\vec{w}(t)$. This ambiguity can be resolved by determining the quadrants for $\alpha(t_k)$ and $\beta(t_k)$ using the $\tan^{-1}(\cdot)$ function over the exact values of $\phi_1(t)$ for $t \in \{t_k, t_{k+1}, t_{k+2}\}$, using (5) – (6).

Using the above formulation, we can estimate $\vec{w}(t_k)$ for multiple zero-crossing instants. Notice that A_2 can be estimated as an average over K zero-crossings, i.e.

$$\hat{A}_2 = \frac{1}{K}\sum_k \sqrt{\|\vec{w}(t_k)\|^2 - 1}.$$

Furthermore, to obtain the Doppler frequencies and phases, we can use the Lomb-Scargle periodogram and complex correlation over the non-uniformly spaced samples of the cosines, as in the Section II-B.

Now, when using the sampled version of $r(t)$, the exact zero-crossing instants of $r(t)$ are not known. Using the estimation approach given in Section III-A, from (3) and (6), the deviation in the value of $\phi_1(\cdot)$ caused due to the lack of knowledge of the precise zero-crossing instants is at most $\pm\pi f_{c1}/f_s$. This would produce errors in the solutions for $\cos\alpha(t)$ and $\cos\beta(t)$ due to the jitter in t_k that affects equations (6) and (10). To obtain a bound on the error in $\vec{w}(t)$ introduced due to the coarse sampling, we conduct a perturbation analysis on $(M(t), \vec{w}(t))$, using the equations $M(t)\vec{w}(t) = 0$ and $|w_1(t)|^2 + |w_2(t)|^2 = 1$. Denoting the time uncertainty induced jitter in $M(t)$ as $\Delta M(t)$ and the propagation of the error as $\Delta\vec{w}(t)$, we obtain

$$\big(M(t) + \Delta M(t)\big)\big(\vec{w}(t) + \Delta\vec{w}(t)\big) = \vec{0}.$$

Neglecting the second order term $\Delta M(t)\Delta\vec{w}(t)$, and substituting $M(t)\vec{w}(t) = \vec{0}$, we obtain

$$M(t)\left(\Delta\vec{w}(t)\right) = -\Delta M(t)\,\vec{w}(t). \tag{11}$$

With $g(\vec{w}(t)) \triangleq |w_1(t)|^2 + |w_2(t)|^2$, the non-linear constraint $g(\vec{w}(t)) = 1$ implies that the error vector $\Delta\vec{w}(t)$ is orthogonal to the gradient of the constraint, i.e., $\nabla g(\vec{w}(t))^T\Delta\vec{w}(t) = 0$. Stacking this with (11), we get

$$\begin{bmatrix} M(t) \\ \nabla g(\vec{w}(t))^T \end{bmatrix}\Delta\vec{w}(t) = \begin{bmatrix} -\Delta M(t)\vec{w}(t) \\ 0 \end{bmatrix}. \tag{12}$$

From this we can bound the error in $\vec{w}(t)$ as

$$\|\Delta\vec{w}(t)\|_F \leq \left\| \begin{bmatrix} M(t) \\ \nabla g(\vec{w}(t))^T \end{bmatrix}^{-1} \right\|_F \|\Delta M(t)\|_F \|\vec{w}(t)\|_F,$$

where $\|\cdot\|_F$ denotes the Frobenius norm. The Frobenius norm of the error vector, $\|\Delta\vec{w}(t)\|_F$, represents the error power due to jitter, which, in addition to the noise power, determines the average distortion power across entire Lomb-Scargle periodogram. An increase in this norm leads to a proportional degradation in the peak SNR, thereby increasing the statistical variance of the estimated Doppler frequency f_d.

One approach to limit this error would be to obtain the solutions by dithering all the zero-crossing points uniformly and independently at random within $[t'_k - \frac{1}{2f_s}, t'_k + \frac{1}{2f_s}]$, where t'_k is the mid-point between the two sample points within which a zero-crossing occurs. We then choose the estimate of $\vec{w}(t_k)$ that yields the least sum of squared residuals in the estimation of $\{\phi_1(t_k), \phi_1(t_{k+1}), \phi_1(t_{k+2})\}$ over disjoint tuples of $\{k, k+1, k+2\}$. This would allow us to select $\{\hat{\phi}_1(t_k), \hat{\phi}_1(t_k+1), \hat{\phi}_1(t_{k+2})\}$ that are much closer to the accurate solution with a high probability. Here, we choose the solution that minimizes the residual error among N independently and uniformly distributed values of $\{t_k, t_{k+1}, t_{k+2}\}$. This reduces the uncertainty in $M(t)$. Specifically, the error bound $||\Delta M(t)||$ scales inversely with the number of dithering samples N, thereby tightening the maximum error bound of the vector $\vec{w}(t)$. In the absence of noise, with $N \to \infty$, the error $\|\Delta\vec{w}(t)\|_F$ diminishes and gives accurate f_d. In other words, the error drops and is simply reduced to the remaining ambiguity among the solutions that give zero-residual, which are few in number. However, this leads to an increase in operational-complexity by a factor of N, resulting in overall time-complexity to be $O(N \cdot K \cdot F_{\text{search}})$.

Algorithm 1 Introducing dithering to reduce residual error in calculation of $\vec{w}(t_k)$ for all k

```
Input: Received signal r[n], carrier frequencies f_c1, f_c2
Output: Doppler shifts f_d1, f_d2 & phase shifts θ1, θ2
for k = 0 to K do
  for i = 1 to N do
      {Here, N is number of dithering samples}
    Calculate {t'_k, t'_{k+1}, t'_{k+2}} as mid-point of transitions
    Generate δt_l ~ U(-1/(2f_s), 1/(2f_s)) for l ∈ {k, k+1, k+2}
    t_l ← t'_l + δt_l for l ∈ {k, k+1, k+2}
    Estimate w(t_k) for the above {t_k, t_{k+1}, t_{k+2}}
    Calculate sum of squared residual error in the equation M(t)w(t) = 0
    Choose {t_k, t_{k+1}, t_{k+2}} and w(t_k) with least error
    k ← k + 3
  end for
end for
Use Lomb-Scargle on w(t_k) for all k to obtain (f_d1, θ1) and (f_d2, θ2).
return (f_d1, θ1), (f_d2, θ2)
```

IV. Simulation Results

We have simulated the proposed approaches and have quantified their benefits in terms of frequency estimation accuracy. We denote the error in frequency estimation for single carrier as $\tilde{f}_d = f_d - \hat{f}_d$ where $\hat{f}_d$ represents the estimated value and f_d is the true Doppler shift. The signal is assumed to have two carriers that arrive at the receiver with channel effects being reflected as changes in their amplitudes and phases. The received signal is affected by additive white Gaussian noise, and is then sampled and quantized using a 1-bit quantizer. We apply our proposed methods on these 1-bit samples and quantify the performance under different noise variances and sampling rates. Table I shows the carrier

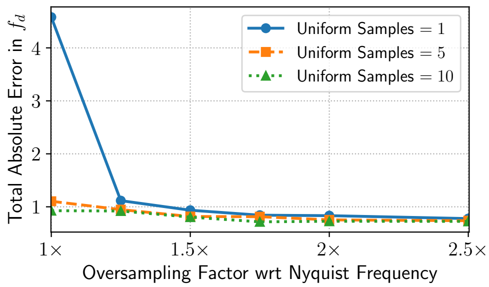

Fig. 2. Sum of absolute errors in Doppler frequency against oversampling factor as a multiple of the Nyquist frequency.

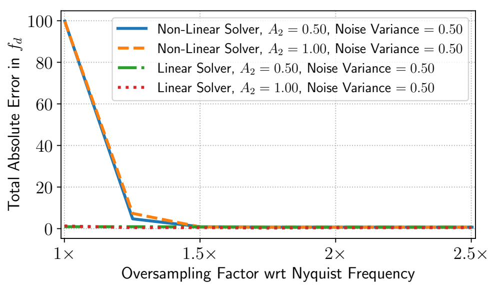

Fig. 3. Sum of absolute errors in Doppler frequency against oversampling factor for different signal strengths and noise variance.

frequencies, phase offsets and amplitudes that we consider for our simulations, and all the inferences are drawn from data accrued over 0.05 s. We employ the linear approach discussed

TABLE I
SIMULATION PARAMETERS

Carrier Frequency	Doppler Frequency	Phase Offset	Amplitude
0.4 MHz	190 Hz	$\pi/3$	1
0.3 MHz	100 Hz	$\pi/6$	0.5

in Section III, wherein we observe the sum of the absolute errors in estimation of frequency deviation, viz. $|\tilde{f}_{d1}| + |\tilde{f}_{d2}|$ for different oversampling factors as a multiple of the Nyquist frequency 0.81 MHz. The error trend against oversampling as a factor of the Nyquist frequency with noise variance as 0.25 is shown in Fig. 2.

The results in Fig. 3 present the results for the linear solver based approach, which involves minimizing the residual over 10 uniformly dithered time offset realizations for 0.1 s. For the non-linear solutions, Lomb-Scargle Periodogram is used for spectral estimation. We observe from Fig. 3 that the linear solver is much more robust to noise and provides high accuracy with very little oversampling. The non-linear solver is affected significantly due to its sensitivity to the initial estimate as well as the impact of local minima in the solution space. Choosing a sampling rate that is co-prime to the frequencies can further reduce the errors in the frequency estimates.

V. CONCLUSION

Carrier recovery in communication systems generally requires the use of high speed ADCs with larger vertical resolutions, that are complex and consume a lot of power. Here, the use of 1-bit ADCs can significantly reduce the cost and complexity. Past work has largely focused on the recovery of a single carrier, while have presented novel methods for simultaneous recovery of two carriers from 1-bit noisy received samples. Our key contribution is that we use the transition information of the 1-bit samples and use spectral estimation to estimate two carriers' frequency offsets, phases, and relative amplitudes simultaneously. Our use of a periodogram based approach scales well to not only provide accurate estimate under noise, but also offers robust performance even at lower sampling rates with inaccurate zero-crossing time estimates. Future work would focus on recovering multiple carriers and Fourier based methods that exploit complex baseband based approaches for carrier recovery with reduced complexity.

REFERENCES

[1] U. Madhow, *Fundamentals of Digital Communication*. Cambridge University Press, 2008.
[2] Z. Liu, A. Bhandari, and B. Clerckx, "λ–MIMO: Massive MIMO via modulo sampling," *IEEE Trans. Commun.*, 2023.
[3] A. Kumar, K. Appaiah, and S. R. B. Pillai, "Carrier phase and frequency discriminators for receivers with one-bit quantization," *IEEE Trans. Commun.*, 2025.
[4] O. Graf, A. Bhandari, and F. Krahmer, "One-bit unlimited sampling," in *ICASSP 2019-2019 IEEE International Conference on Acoustics, Speech and Signal Processing (ICASSP)*. IEEE, 2019, pp. 5102–5106.
[5] A. Eamaz, K. V. Mishra, F. Yeganegi, and M. Soltanalian, "UNO: Unlimited sampling meets one-bit quantization," *IEEE Trans. Signal Process.*, 2024.
[6] C.-F. Chang and M.-S. Kao, "High-accuracy carrier phase discriminator in one-bit quantized software-defined receivers," *IEEE Signal Process. Lett.*, vol. 15, pp. 397–400, 2008.
[7] J. Zhao, J. Zhang, and J. Yin, "A robust digital phase discriminator in one-bit quantized software-defined receivers," in *2009 5th International Conference on Wireless Communications, Networking and Mobile Computing*. IEEE, 2009, pp. 1–4.
[8] C.-F. Chang, R.-M. Yang, and M.-S. Kao, "1-bit high accuracy carrier phase discriminators," *IEEE Trans. Aerosp. Electron. Syst.*, vol. 49, no. 1, pp. 160–174, 2013.
[9] W.-H. Hsieh, C.-F. Chang, and M.-S. Kao, "SNR-aided accurate phase estimation in 1-bit software-defined receiver," *IEEE Trans. Aerosp. Electron. Syst.*, vol. 48, no. 2, pp. 1570–1582, 2012.
[10] C.-F. Chang and N. A. R. Laboratories, "Phase-discriminating device and method," US Patent US8 238 506B2, 2012.
[11] Y. Ye, H. Xiao, and G. Xiao, "A Rotation-Aided Arctangent Phase Discriminator With One-Bit Quantization," *IEEE Signal Process. Lett.*, vol. 23, no. 9, pp. 1236–1240, 2016.
[12] J. N. Laska, Z. Wen, W. Yin, and R. G. Baraniuk, "Trust, but verify: Fast and accurate signal recovery from 1-bit compressive measurements," *IEEE Trans. Signal Process.*, vol. 59, no. 11, pp. 5289–5301, 2011.
[13] D. M. Akos, A. Ene, and J. Thor, "A prototyping platform for multi-frequency gnss receivers," in *Proceedings of the 16th International Technical Meeting of the Satellite Division of The Institute of Navigation (ION GPS/GNSS 2003)*, 2003, pp. 117–128.
[14] J. Huang, R. Yang, and X. Zhan, "Cross-band correlator and detector design for robust gnss multifrequency combined acquisition," *IEEE Trans. Aerosp. Electron. Syst.*, vol. 59, no. 1, pp. 720–733, 2022.
[15] M. B. Djurić and Ž. R. Djurišić, "Frequency measurement of distorted signals using Fourier and zero crossing techniques," *Electric Power Systems Research*, vol. 78, no. 8, pp. 1407–1415, 2008.
[16] V. Friedman, "A zero crossing algorithm for the estimation of the frequency of a single sinusoid in white noise," *IEEE Trans. Signal Process.*, vol. 42, no. 6, pp. 1565–1569, 1994.
[17] J. T. VanderPlas, "Understanding the lomb–scargle periodogram," *The Astrophysical Journal Supplement Series*, vol. 236, no. 1, p. 16, 2018.
[18] P. Virtanen, R. Gommers, T. E. Oliphant, M. Haberland, T. Reddy *et al.*, "SciPy 1.0: Fundamental algorithms for scientific computing in Python," *Nature Methods*, vol. 17, no. 3, pp. 261–272, 2020.